

# CONSTRUCTION OF A PRACTICAL FINITE ELEMENT MODEL FROM POINT CLOUD DATA FOR AN EXISTING STEEL TRUSS BRIDGE

*Nao Hidaka, Naofumi Hashimoto, Tetsuya Nonaka & Makoto Obata*  
Nagoya Institute of Technology, Japan

*Kazuya Magoshi*  
Earthquake Engineering Research Center Inc., Japan

*Ei Watanabe*  
Aichi Prefectural Government, Japan

**ABSTRACT:** *The objective of this paper is to develop a semi-automatic method for constructing a practical finite element model from point cloud data of an entire span of a through-type steel truss bridge. In the first step, we introduced practical finite element models for truss bridges based on structural experiments and numerical analyses of a sway bracing located at the end support. We also proposed a basic method for semi-automatically constructing a finite element model of a sway bracing using point cloud data. This method was then extended for an entire of steel truss bridge. The point cloud data is converted to individual data structures which, in turn, are connected to construct a whole structure. The main members, such as upper chords, lower chords, and diagonals, are converted to fiber-based models by automatically creating central axis lines and cross-sections from the point cloud. The slab is converted to shell models by obtaining surfaces and thickness from the point cloud. The effectiveness of the proposed method was confirmed by comparing the analysis results from the finite element model manually created from the design drawing (drawing-model) with those obtained from the model generated by this method (point-cloud-model). The proposed method is more efficient than reading drawings and creating the models manually, and it was confirmed that the point-cloud-model shows response values close to those of the drawing-model within the design load. However, the reproducibility of the response values with more than the design load remains an issue, which can be solved by tuning plate thickness.*

**KEYWORDS:** *Point Cloud, Fiber-based model, Steel Truss Bridge, Structural Analysis Model, Semi-Automatic Method*

## 1. INTRODUCTION

A vast number of existing bridges are rapidly aging. Since it is not practical to rebuild all of them at the same time, strategic renewal through life cycle extension is required. To extend the life cycle of bridges, quantitative evaluation of the residual load capacity is being promoted through numerical analysis. The accuracy of the analytical model, such as finite element model configuration (dimensions, materials, and boundary conditions) has been verified through structural experiments and is now being realized with high reproducibility (Magoshi et al. 2014), but the efficiency of the generation method still remains an issue.

Construction of a finite element model requires acquisition of member dimensions of a target structure. However, in cases of old bridges, as-build drawings are often unavailable. In addition, conditions of bridges inevitably changed since its construction due to various factors. Therefore, it is necessary to construct a finite element model based on dimensions data instead of relying on drawings, but manual measurement is time-consuming and prone to various human errors.

Therefore, a method to efficiently construct a finite element model from point cloud data, which can efficiently reproduce the 3D shape of an object, has begun to attract attention. Some existing methods (Suzuki et al. 2019 and Nakamizo et al. 2022) convert point cloud data to a finite element model by shell or solid elements, but the shell or solid element models are not practical because of their computational burdens. In addition, such methods are only applicable to simple structures like simple beams and not to usual structures consisting of multiple members. Therefore, it is necessary to apply structures with multiple members connected to each other and to convert to fiber-based models used in practice. Fig. 1 shows a type and outline of finite element models.

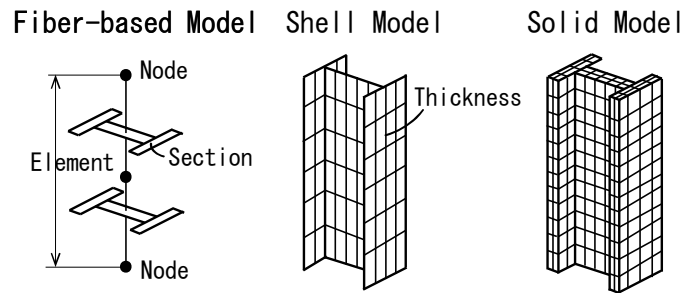


Fig. 1: The types of finite element models used in structural mechanics

The authors have developed a method for constructing a fiber-based model from point cloud data and applied a case of sway bracing located at the end support of a steel truss bridge in the structural experiment (Hidaka et al., 2023). The numerical result based on the fiber-based model constructed by the proposed method reproduced the experimental result very well. It is interesting to note that the model yields a better result than an analytical model manually constructed from the drawings. The point cloud based model can reflect accurately the state of a structure as it is. A real structure cannot avoid initial imperfections within tolerance.

In this paper, the modeling method is extended to a whole truss bridge. A semi-automatic procedure is proposed and developed to construct a finite element model from the point cloud data of the entire side span of a through-type truss bridge. To verify the validity of the model, a model created manually from drawings was also prepared, and the response values were compared under the same loading conditions.

## 2. CASE STUDY

A two-span continuous through-type truss bridge in Aichi Prefecture, Japan, was measured in March 2023. A photograph of the bridge is shown in Fig. 2(a). The bridge length is 136.9m with a span length of 2@67.9m. A full width is 14.3 m with sidewalks on both sides. The effective width of the roadway is 7.5 m and that of the sidewalk is 2.0 m without width widening. A slab thickness is 200 mm with a pavement of 80 mm thickness (roadway) and of 30 mm thickness (sidewalk). In addition, the bridge is straight and has a symmetric cross slope. A general bridge drawing is shown in Fig. 2(b).

In acquisition of point cloud data of the entire P4-A2 span, the stationary laser scanner (Leica RTC360, resolution: 3mm@10m, accuracy: 1.9mm@10m) was used from the beneath of the girder and from the road surface. The number of points in the point cloud was about 1 billion. Furthermore, the handheld laser scanner (HandySCAN BLACK™ Elite, resolution: 0.05 mm@30 cm, accuracy: 0.025 mm@30 cm) was used to measure the detailed geometry of the parts of lower chords, braces, main girders, and lower lateral bracing. The lower chord, main girder, and lower lateral bracing were measured for the member closest to the abutment due to on-site restrictions, and two braces (two different cross-sectional shapes) were measured for the member closest to the pier (fixed bearing). The number of points in each point cloud was approximately 0.3 to 1.5 million. The point cloud data is shown in Fig. 2(c). The total measurement time was approximately 3 hours. The coordinate system was set so that the x-axis is along the longitudinal direction, the y-axis is transverse direction, and the z-axis is along the height direction. Table 1 shows the dimensions of each member components. Measured values, data in the as-built drawings and data by the handheld laser scanner are given.

The bridge is a two-span continuous bridge, but due to on-site restrictions, only P4-A2 span were measured; to interpolate the parameter of P3-P4 span, the altitudes of fulcrum at both ends were measured with a total station.

## 3. PROPOSED METHOD

A computer program is developed to generate fiber-based models for numerical analysis from point cloud data obtained in Chapter 2. To construct a fiber-based model, nodes along an axis passing through a center of each member, elements connecting the nodes, a cross-sectional geometry of each element, and other material and loading conditions are required.

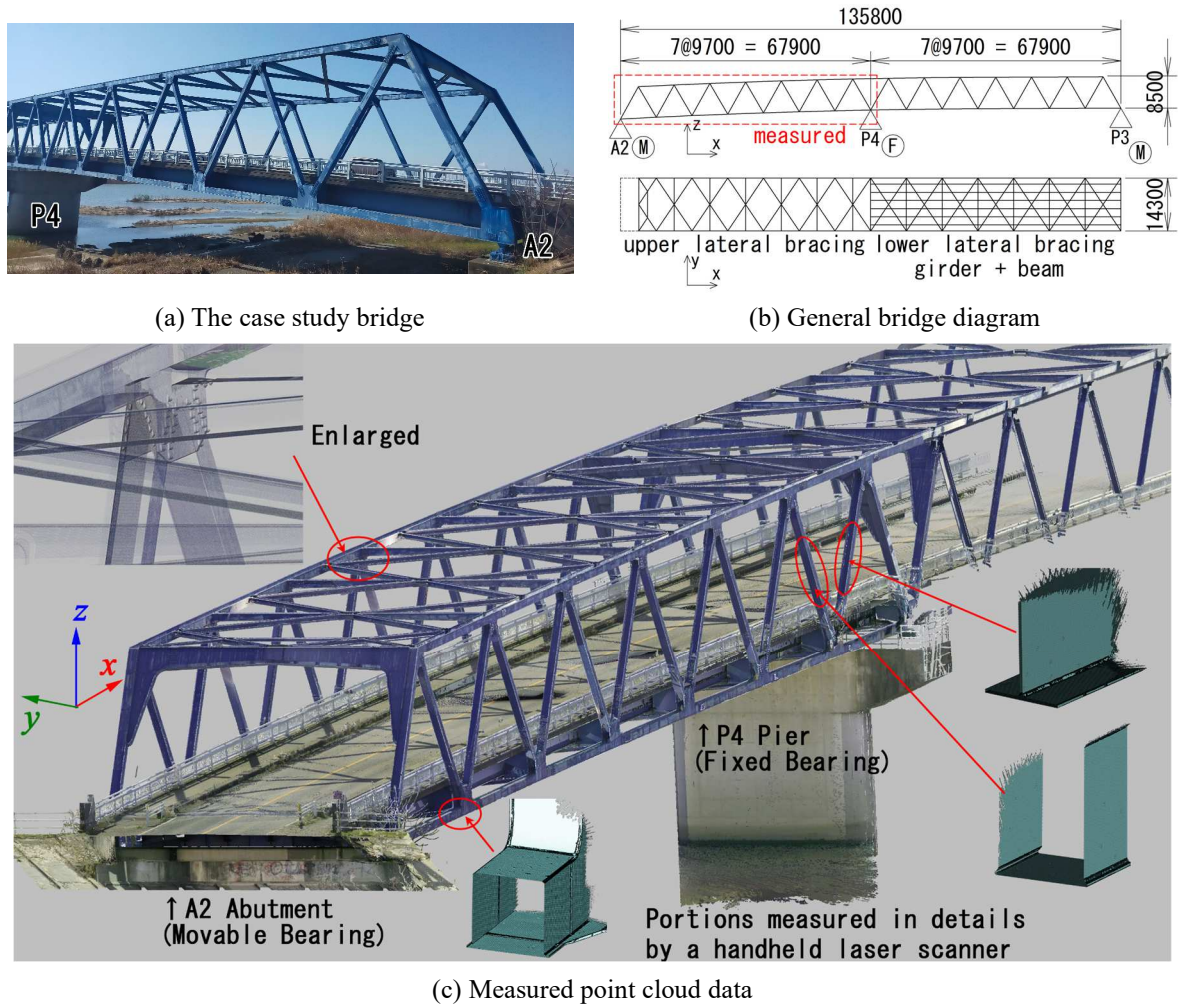


Fig. 2: The case study bridge and measured point cloud data

Table 1: Arrangement of measured dimensions of bridges

		Lower chord			Brace (Compression)			Brace (Tension)			Main girder			Lower lateral bracing			
Cross section																	
		D	M	H	D	M	H	D	M	H	D	M	H	D	M	H	
Length	Flg.	U	380	379.1	380.8	350	351.0	351.1	350	352.0	351.2	230	230.0	230.2	360	361.0	360.9
		L	460	462.3	461.8												
		Web	380	378.0	379.1	340	339.1	340.7	322	324.0	—	1000	1002.3	—	180	180.3	180.6
Thick ness	Flg.	U	9	—	8.5	19	19.4	19.3	22	22.5	22.4	14	14.2	14.2	19	19.5	19.3
		L	10	11.1	10.6												
		Web	11	11.3	10.9												

(Unit: mm)

D: as-built drawings, M: manual measured, H: handheld laser scanner, U: upper, L: lower, -: not measurable

### 3.1 Creating nodes and elements for a fiber-based model from a point cloud

In the first step, nodes and elements are created from point cloud data. In this step, taking advantage of the fact that braces of the truss bridge are connected to many members (such as upper and lower chords, upper and lower lateral bracings, and cross beams), nodes, the central axes of the braces are extracted from the point cloud data of the entire bridge, and the nodes and elements of the fiber-based model are created by making the points of intersection between the central axes of adjacent braces as grid points.

First, point cloud data of the entire bridge (Fig. 3(a)) is sliced along a longitudinal direction (in this case, the x-axis direction) from an abutment position at small intervals. A cross-sectional point cloud is obtained as shown in Fig. 3(b). By grouping points in the cross-sectional point cloud based on the Euclidean distance (Ester et al., 1996), point groups of cross sections of each member (such as upper and lower chords) are separated. Centroids of these cross sections correspond to a center axis of each member, and if continuing to slice, candidate points for the center axis of the members are created as shown in Fig. 3(c). If location of centroid is obtained by a simple average method, it is biased by the density of point cloud data. To avoid the bias, cross-sectional point cloud is converted to polyline with the convex hull (Preparata and Hong, 1977) method and a centroid is obtained using an image processing algorithm.

Next, central axes are obtained from the candidate points for the center axis using the RANSAC method (Fischler and Robert, 1981). In the above procedure, however, central axes of other members than braces are inevitably included. The central axes of braces can be extracted by using a threshold value method based on the fact that they extend in the x- and z- directions. To create intersections of the central axes of the adjacent braces, the central axes are sorted as x-coordinates of the center points in the axes. When the two lines are in a twisted position, the intersection is defined here as a midpoint of a line segment that is orthogonal to two lines and has the shortest length. After creating the grid points, nodes are sampled at equally spaced intervals along the line segment connecting the two grid points, with the specified number of nodes. For the upper lateral bracing, its grid points are located at the center of the upper chords.

Since grid points, nodes, and elements of main girders cannot be created from grid point of braces, they are created additionally. Fig.4 shows a summary to create grid points of main girders. A cross-sectional point cloud perpendicular to longitudinal direction at a location of a cross beam is obtained. Points within 1 m of the upper side of a line connecting grid points of lower chords (bottom horizontal line in Fig. 4) are extracted and divided into point groups of main girders and others based on Euclidean distance. To extract main girder lines, the divided point groups are converted into direction vectors by using principal component analysis and only the z- direction vectors are extracted as main girder lines (blue vertical lines in Fig. 4). Intersections of main girder lines and a line connecting grid points of lower chords are grid points of the main girders. To account for the possibility that grid points cannot be created at a few of cross beam positions, the average value of the created grid points was calculated. After creating grid points, if there is a cross beam position where the grid points cannot be generated by the above procedure, the calculated average value is applied.

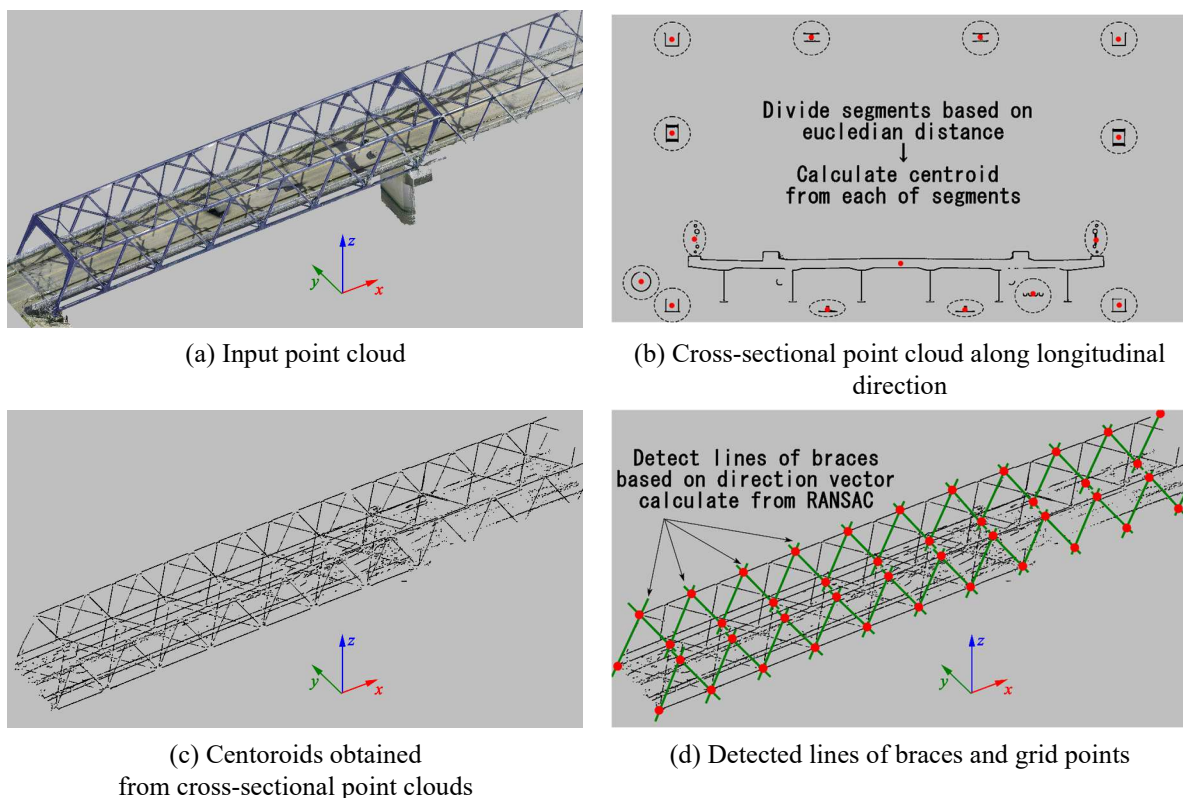


Fig. 3: Creating grid points of braces by using cross-sections and centroids

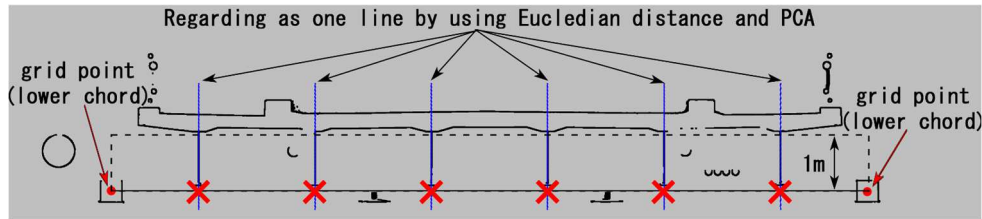


Fig. 4: Creating grid points of main girders (cross mark is a grid point)

### 3.2 Obtaining a cross-sectional geometry of each member for a fiber-based model from a point cloud

In the second step, once the nodes and the elements have been created, the next step is to obtain a cross-sectional geometry to be applied to the elements. In finite element models, a cross-sectional geometry is represented by a collection of rectangles as shown in Fig. 5. The rectangle is defined by the coordinates of a start and an end point and its thickness. The coordinate system of the cross section must be converted to a two-dimensional coordinate system (such as u-v coordinate system) with the origin at the position through which the element axis lines pass.

Cross-sectional geometry is obtained using cross-sectional point cloud perpendicular to a direction vector of the element passing through the midpoint of the element. Because point cloud measured by the stationary laser scanner (accuracy: 1.9mm@10m) is difficult to ensure accuracy of plate thickness, representative cross-sectional geometry is obtained from the point cloud data measured by the handheld laser scanner (accuracy: 0.025 mm@30 cm), and is applied to all the elements of the corresponding member. In addition, for the upper chords, the upper lateral bracing, and the cross beams which could not be measured by the handheld scanner due to on-site restrictions, the vertical and horizontal scales of cross sections of other members with similar shapes were adjusted. Specifically, the cross-sectional geometry of the upper chords is a vertically inverted that of the lower chords, the upper lateral bracing applies the I-section of the braces, and the cross beam applies to the cross-sectional geometry of the main girder. Table 2 shows the relation of them. For members whose entire surface could not be measure by the handheld laser scanner due to on-site restrictions, the symmetric center point of the cross-section at the same position was obtained from the point cloud data collected by a stationary laser scanner. Subsequently, the cross-sectional geometry was determined by duplicating the measured portion through rotational symmetry, utilizing the point symmetry of the cross section. In the following, the methods of obtaining cross-sectional geometry are explained according to the type of geometry.

Table 2: The relation of applying cross-sectional geometry of members that could not be measured by the handheld laser scanner

Unscanned member	Upper chord	Upper lateral bracing	Cross beam
Referenced member	Lower chord	Brace (Tension)	Main girder
Cross section			

#### 3.2.1 Open cross-section (I-shape and T-shape)

Midpoints of all point pairs in a cross-sectional point cloud are created (Fig. 6(a)), and the midpoints that are not on the cross-sectional point cloud are extracted as points of candidate centerlines. These are converted to straight lines by using RANSAC (Fig. 6(b)), intersection points of these lines and the cross-sectional point cloud are starting and ending points (Fig. 6(d)), and its thickness is obtained by doubling an average of the shortest distances from the cross-sectional point cloud (Fig. 6(c)).

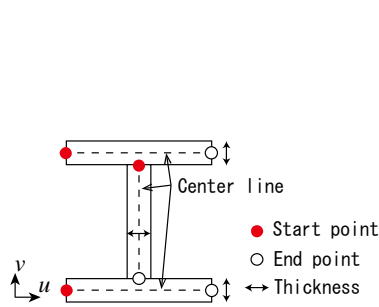


Fig. 5: Parameters of section for fiber-based model

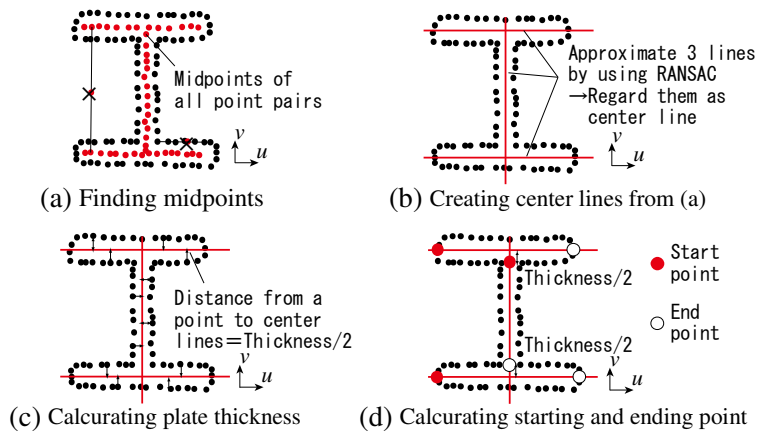
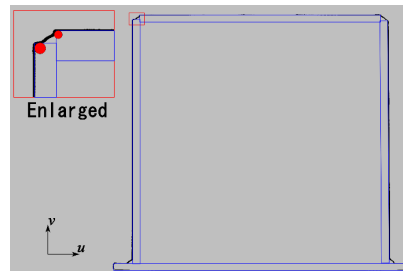
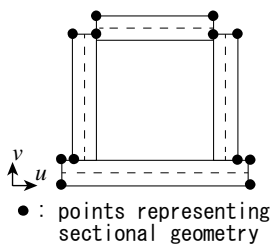


Fig.6: Obtaining parameters of open-cross section

### 3.2.2 Close cross-section (quadrangle-shape)

The algorithm in 3.2.1 cannot be applied to a square cross section because back sides of plates cannot be measured. Therefore, as shown in Fig. 7(a), cross-sectional geometry is constructed by finding points at corners. Since corner points and joint positions are rounded, as shown in Fig. 7(b), corner points can be found by taking a local area at all points of the cross section and extracting the area where the radius of the circle is smaller when fitting it to a circle. For areas where thickness cannot be measured, such as the web and the upper flange of the lower chord, general plate thicknesses are used.



(a) Cross-sectional geometry of quadrangle-shape (b) Finding corner points by fitting to circles  
 Fig.7: Getting parameters of close-cross section

### 3.3 Creating a slab model as a shell model

Only in a case of modeling for a slab, to reproduce load sharing of live load accurately, a shell model is constructed. It is connected to main girders and cross beams in the fiber-based model with springs. As shown in Fig. 8, a position of a slab is determined by finding the difference in z-coordinates between the main girder grid points and a centerline of the slab, and offsetting the z-coordinates from the main girder grid points by that value. In the same way as in Sec. 3.2.1, a centerline of a slab is obtained by finding midpoints of all point pairs in a cross-sectional point cloud of a slab and extracting points of a candidate centerline that are not on the cross-sectional point cloud. This is converted to a straight line, and the average of the shortest distances from the cross-sectional point cloud of the slab is doubled to obtain the slab thickness. As the slab thickness obtained in the above procedure includes the pavement portion, the thickness after subtracting a typical pavement thickness of 80mm is used.

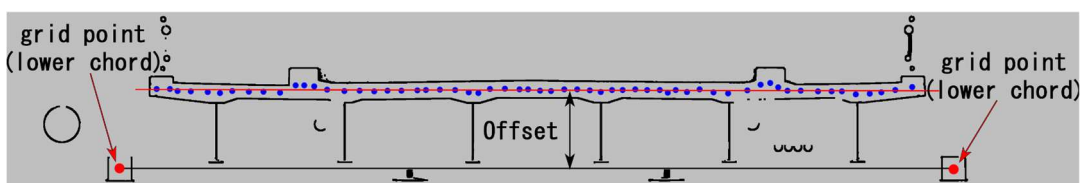


Fig. 8: Obtaining offset and thickness parameter of a slab

### 3.4 Implementation

The proposed methods were applied to the point cloud data in Chapter 2. Due to memory limitations, the point cloud data measured by the stationary laser scanner was down-sampled from approximately 1 billion points to approximately 200 million points (3 mm pitch). Only the nodes and elements in P4-A2 span were created from the point cloud data, and those in P3-P4 span were extrapolated by duplicating the linearly stored height of the grid using the altitudes of fulcrum difference. Table 3 shows the development environment.

The program that implements the proposed method is divided into several phases because it requires several manual operations in the process. The program flow is shown in Fig. 9.

Table 3: Development Environment

CPU	Intel(R) Xeon(R) Silver 4214R CPU @ 2.40GHz 2.39 GHz (2 processors)
Memory	64GB
GPU	NVIDIA GeForce RTX 3080 (10GB)
OS	Windows 10 Enterprise 22H2 64bit
Development Environment	Microsoft Visual Studio Community 2022 64bit
Library	Point Cloud Library (PCL) 1.12.0 64bit (Rusu, 2011), OpenCV 4.5.5 64bit
Programming Language	C++
Structural analysis software	SeanFEM (Earthquake Engineering Research Center Inc., 2007)

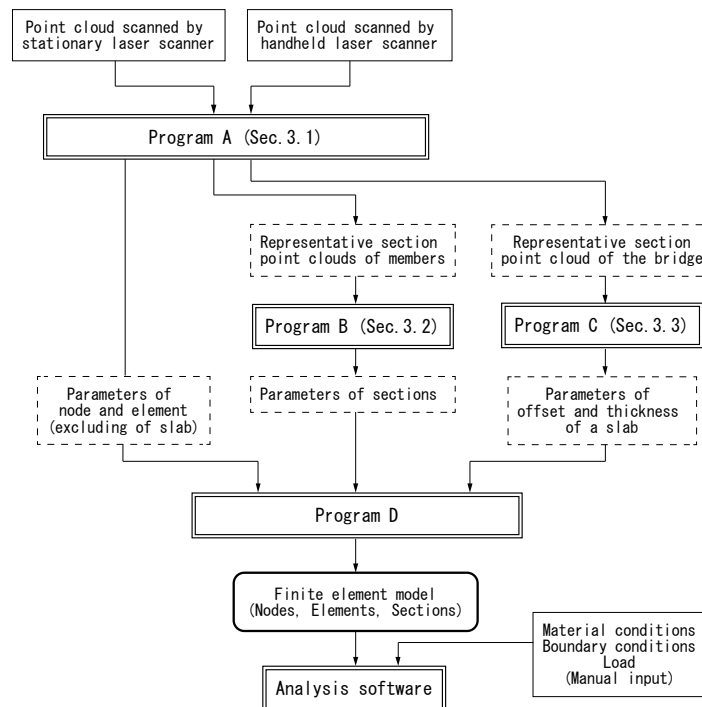


Fig. 9: The flow of implement for the proposed method

First, the nodes and the elements excluding for slab are obtained by inputting the point cloud measured by the stationary laser scanner and the handheld laser scanner into Program A, which performs the procedure described in Sec. 3.1. To obtain the cross-sectional geometries, the representative cross-sectional point cloud of each member is output. Furthermore, to obtain the nodes and the elements of the slab, the representative cross-sectional point cloud of the bridge perpendicular to longitudinal direction is output.

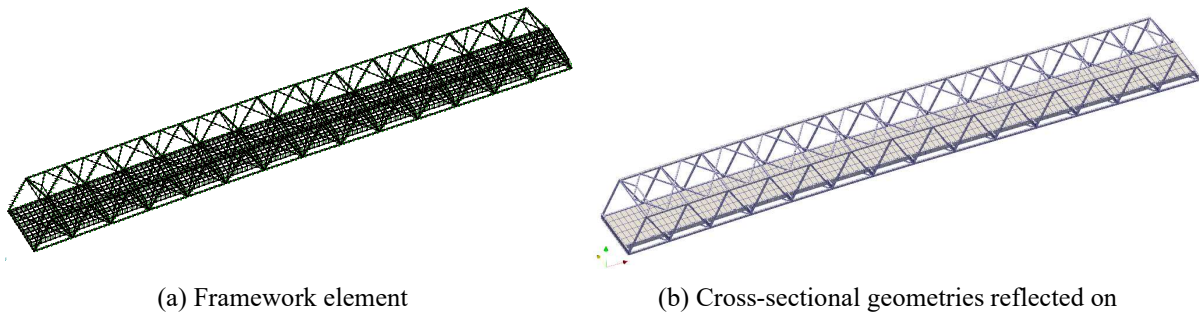
Next, in order to obtain the cross-sectional geometry, the missing part is manually compensated, and the scale is adjusted to apply to other members. After that, they are input to Program B, which performs the processing described in Sec. 3.2.

After the slab points are manually extracted from the cross-sectional point cloud data, they are input into Program C that performs the procedure described in Sec. 3.3.

Finally, the output results of Programs A, B, and C are input to Program D, which outputs the finite element model. Once the nodes, elements and cross-sections are obtained in this way, the material and boundary conditions are manually specified and entered into the analysis software.

Excluding manual operations such as preliminary down-sampling and correction of missing points in the cross-sectional point cloud, it took 35 minutes to input the stationary laser scanner point cloud, create the KD search tree, slice the cross-section in the 100 mm pitch in the longitudinal direction, divide them using the Euclidean distance, and obtain the centroid of each member cross-section. In addition, it took 1 minute to extract the central axis of the braces from the point cloud of the centroid, 6.5 minutes to obtain the grid point position of the main girder, and 1 minute per section to obtain the end point and plate thickness of the cross section. The remaining processing was completed in less than 1 second.

The generated finite element model is shown in Figs. 10. (a) is the framework element, and (b) is the cross-sectional geometries reflected on it.



(a) Framework element (b) Cross-sectional geometries reflected on  
 Fig. 10: The analysis model from point cloud by using the proposed method

## 4. RESULTS AND DISCUSSION

### 4.1 Results of repeatability analysis

The response values of nonlinear analysis were analyzed by applying progressively increasing dead and live load according to the Japanese Specification for Highway Bridges (Japan Road Association, 2017). Dead load is loaded to whole of the bridge and live load is loaded as Fig. 11. The material conditions and reinforcement of the slab were set based on actual bridge design experience. To verify the validity of the model, the same loading conditions were applied to a model created manually from drawings. Hereafter, the finite element model generated by the proposed method will be referred to as the "point-cloud-model" and the model from the drawing as the "drawing-model".

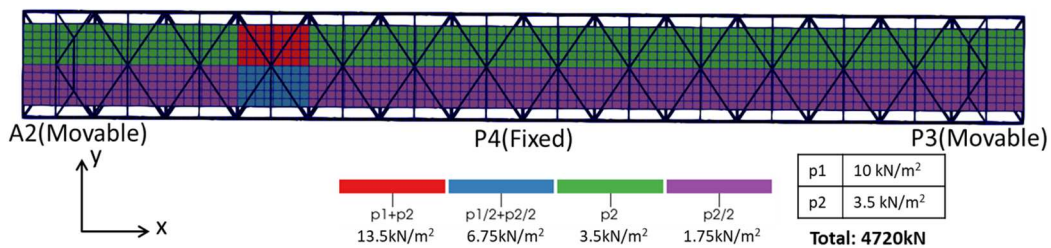


Fig. 11: Live load

The displacement of the point-cloud-model was close to that of the drawing-model within the design load that is the sum of dead and live load. Additionally, when examining the strain contour and deformation diagrams for the design load (Fig. 12), the deflection of the bridge exhibited a nearly identical behavior between the two models. However, with a load larger than the design load, the response value of point-cloud-model was different to the drawing-model (Fig. 13(a)). As the deformation diagram of the point-cloud-model for the 1.3 times of the design load (Fig. 13(b)), one upper chord at left-side in the center span of P4-A2 was extremely deflected. Consequently, a discernible variance arose between the response of the point-cloud model and that of the drawing model.

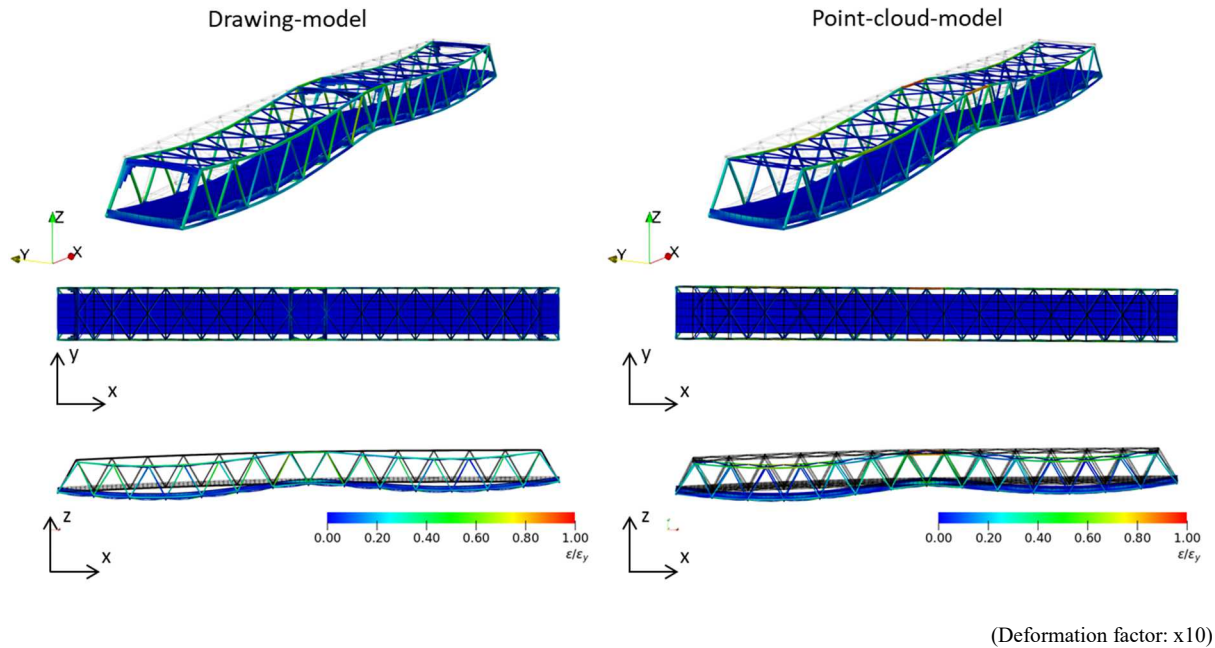
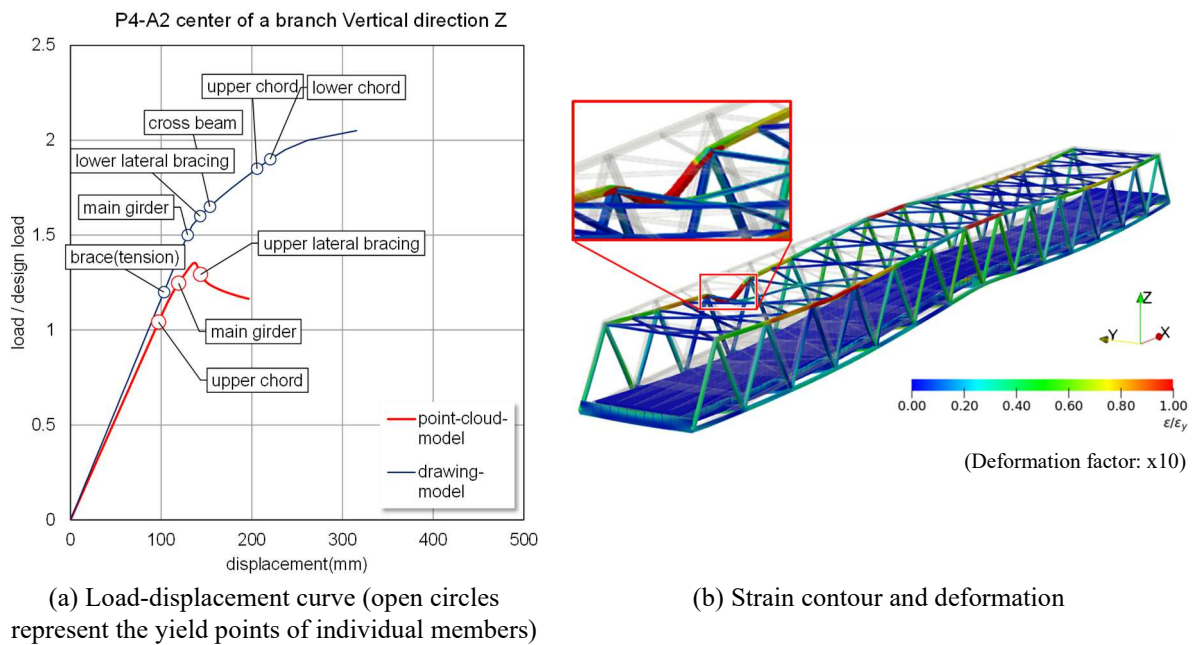


Fig. 12: Strain contour and deformation for the design load



(a) Load-displacement curve (open circles represent the yield points of individual members)

(b) Strain contour and deformation

Fig. 13: Response value for the 1.3 times of the design load

## 4.2 Discussion

To improve maintenance efficiency, a method was developed to semi-automatically construct a fiber-based model (the slab is a shell model) that reproduces the structure of a truss bridge from point cloud data. When the drawing-model was created manually from drawings, it took several days to read the dimensions and connections of the members and input them into the software. In particular, the most time-consuming step was the input of cross-sectional geometries due to variations in plate thickness. The point-cloud-model, on the other hand, took about three hours to measure the point cloud data and less than one hour to generate the model from the point cloud data. Other manual work, such as processing noise and filling missing portions in the cross-sectional point cloud, can still be completed in 12 to 24 hours. The proposed method is expected to contribute to efficient maintenance and management.

However, there are several issues related to the accuracy of elemental axis construction and the limits to applicable structures.

The point-cloud-model demonstrated a response closely aligned with the drawing-model under the design load. However, deviations emerged with a load larger than the design load. One plausible explanation stems from the inherent variability in plate thicknesses and member dimensions among upper chords, lower chords, braces, and lower lateral bracings unlike the brace panel in the previous research (Hidaka et al., 2023). The point-cloud-model encompasses disparities in cross-sectional geometries, as the stationary laser scanner's limited measurement precision and the handheld laser scanner's constrained range preclude the complete capture of all such geometries. Notably, the upper chord's cross-sectional geometry, pivotal for truss bridges experiencing significant forces, eludes handheld scanner measurement and significantly influences analytical outcomes, as evident in Fig. 13(b). Furthermore, the substitution of a representative, thinner cross-sectional geometry for the braces at the span's center, as described in Fig. 14(a), led to a marked reduction in overall bridge stiffness (Fig. 14(b)). These findings underscore the notion that a uniform approach to determining cross-sectional geometries across members with varying plate thicknesses sacrifices precision. Thus, an enhanced methodology is imperative to refine cross-sectional geometries and achieve heightened accuracy.

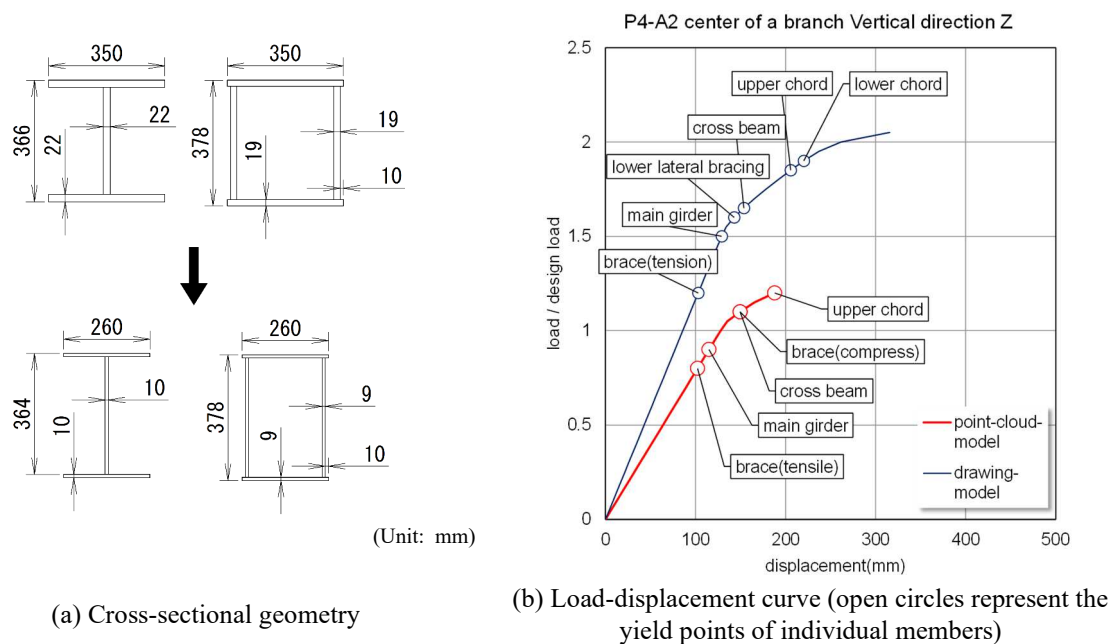


Fig. 14: The case of braces with thinner cross-sectional geometry

In the previous research (Hidaka et al., 2023), the fiber-based modeling approach was employed for simulating sway bracing. This involved adjusting node positions to accurately replicate member bending by utilizing centroids within localized regions. The incorporation of this technique successfully accounted for initial irregularities, resulting in a response that closely aligned with the actual structural behavior. However, in the present case, this method couldn't be employed due to its limited accuracy in centroid generation. This limitation stemmed from numerous factors, including the presence of numerous gaps in the point cloud data as well as the inclusion of extraneous points within local regions intended for centroid calculation. As such, there exists a pressing need to enhance the methodology in order to effectively surmount the aforementioned challenges. The proposed method is based on an algorithm that uses advantage of the fact that the bridge is a straight and has no widening and same truss spanning. It is required to improve the method to extend to curved or width extension bridges. A longitudinal direction of curved bridges and width widening may be obtained by tracing line of curb stones and white lines, for example. In addition, it may be effective to supple missing geometries and dimensions by using information of similar bridges.

## 5. CONCLUSIONS AND FUTURE WORK

In this paper, a method is proposed to semi-automatically generate a finite element model for practical use from a point cloud data for the entire of steel truss bridge without using drawings. The findings are as follows:

- The method to accurately obtain the geometry and member dimensions of the entire bridge was proposed by using stationary and handheld laser scanners.

- A program to construct a finite element model from a point cloud data was developed and its usefulness was demonstrated.
- The proposed method showed the response value is close to the drawing model within the design load, but it is required to improve detailed analysis results with more than the design load. A possible reason for this is that the representative section was uniformly determined for members although they have non-uniform thickness.

In the future, we will address the issues of dealing with various plate thickness and curved bridges, and interpolation of unmeasured points using other dimension data and other parameters, such as road alignment. In particular, for applying appropriate cross-sectional geometries, the following two proposals are seen to be effective and will be implemented.

- A method to determine appropriate members for measurement by using a handheld scanner will be developed. It is useful to estimate the members that are subjected to large cross-sectional forces according to the structural characteristics of a bridge type and span. Additionally, numerical analysis enables us to determine the members whose cross-sectional dimensions require high accuracy, such as the upper chords and diagonals in this particular project.
- We are in the process of devising a methodology to extrapolate cross-sectional geometries from point cloud data measured by a stationary laser scanner. Despite the inherent precision limitation to a few millimeters associated with the stationary laser scanner's point cloud, it facilitates the extraction of crucial details concerning member classification, cross-sectional profiles, and member lengths. Leveraging this data, an effective approach to determine the suitable plate thickness can be formulated.

## 6. ACKNOWLEDGMENT

This research was supported by JSPS Grant-in-Aid for Scientific Research JP22K20445, Nao Hidaka.

## REFERENCES

- Magoshi, K., Komuro, M., Yamasawa, T., Yui, K., MIHARA, R., Nonaka, T., Yoshioka, T., and Okui, Y., (2014). Dynamic Redundancy Analysis For A Steel Truss Bridge (in Japanese), *Proceedings of The 17th Symposium on Steel Structures and Bridges*.
- Suzuki, S., Miyamori, Y., Saito, T., Yamazaki, T., Dambiibaljir, M., and Mikami, S., (2019). Automated FE Modeling From 3D Point Cloud Model Of A Damaged Steel Structural Member (in Japanese), *Journal of Japan Society of Civil Engineers F3*, 75(2), I\_141-I\_149. doi.org/10.2208/jscejci.75.2\_I\_141
- Nakamizo, T. and Mayuko Nishio, M., (2022). Finite Element Modeling With Shell Element From 3D Point Clouds Of Thin-walled Steel Structural Members (in Japanese), *Intelligence, Informatics and Infrastructure*, 3(J2), 786-794. doi.org/10.11532/jsceiii.3.J2\_786
- Hidaka, N., Hashimoto, N., Nakamura, M., Magoshi, K., Nonaka, T., Obata, M., (2023). Construction analysis model of steel bridge by using point cloud data and accuracy verification (in Japanese), *Journal of structural engineering. A*, 69A, 637-647. doi.org/10.11532/structcivil.69A.637
- Ester, M., Kriegel, H. P., Sander, J., and Xu, X., (1996). A density-based algorithm for discovering clusters in large spatial databases with noise, *Proceedings of the Second International Conference on Knowledge Discovery and Data Mining, Portland, Oregon*, 226-231. dl.acm.org/doi/10.5555/3001460.3001507
- Preparata, F. P. and Hong, S. J., (1977). Convex Hulls of Finite Sets of Points in Two and Three Dimensions, *Communications of the ACM*, 20(2), 87-93. doi.org/10.1016/0020-0190(78)90021-2
- Fischler, M. A. and Robert, C. B., (1981). Random Sample Consensus: A Paradigm for Model Fitting with Applications to Image Analysis and Automated Cartography, *Communications of the ACM*, 24(6), 381-395. doi.org/10.1016/B978-0-08-051581-6.50070-2
- Rusu, R. B. and Cousins, S., (2011). 3D Is Here: Point Cloud Library (PCL), *In 2011 IEEE International Conference on Robotics and Automation (ICRA)*, 1-4. 10.1109/ICRA.2011.5980567

Earthquake Engineering Research Center Inc., Japan, (2007). SeanFEM ver.1.2.3 Theoretical Manual and Verification.

Japan Road Association (2017). Road Bridge Design Specifications (in Japanese). Government Publishing Office.